A

# Al-Azhar Bulletin of Science
## Basic Science Sector

THE OFFICIAL PUBLICATION OF
THE FACULTY OF SCINCE
( MEN , GIRLS &ASSUIT BRANCH )
AL-AZHAR UNIVERSITY
CAIRO, EGYPT

ABSB

*Al-Azhar Bulletin of Science: Section A, Vol. 32, No. 1, (June) 2021, pp. 57-70*
http://doi.10.21608/absb.2021.79764.1121

Al-Azhar Bulletin of Science: Section A

# PECULIARITIES OF U(VI) ADSORPTION FROM ACIDIC SOLUTION USING CHITIN-DERIVED CHITOSAN AS A LOW-PRICED BIO-ADSORBENT

**Khaled A. Abd El-Rahem[a], Mahmoud A. Taher[a], Mahamed F. Cheira[b*]**

[a] *Chemistry department, Faculty of Science, Al-Azhar University, Assiut 71524, Egypt.*
[b] *Nuclear Materials Authority, P.O. Box 530, Maadi, Cairo, Egypt*
* Corresponding Author: mf.farid2008@yahoo.com

Received: 11 June 2021; Revised: 17 June 2021; Accepted: 18 June 2021; Published: 28 Sep 2021

## ABSTRACT

Chitosan (CS) as an inexpensive bio-adsorbent was set by chitin deacetylation using sodium hydroxide. The prepared bio-adsorbent was distinguished via Scanning electron microscopy (SEM), X-ray diffraction (XRD), Energy dispersive spectroscopy (EDX), Brunner-Emmett-Teller surface area (BET) analyzer, and Fourier transform infrared spectroscopy (FTIR). Chitosan implemented for U(VI) adsorption, and the studied parameters that are pH, time of contact, initial concentration, and temperature, were determined by batch technique. The maximum uptake of CS adsorbent is 88.0 mg/g at 200 mg/L initial U(VI) concentration, pH 3.5, and 25 °C. The kinetic information agreed with the pseudo-second-order model, which considered the attendance of chemisorption. The equilibrium of adsorption reaction gained within 50 min, and equilibrium information well satisfaction for Langmuir model confirmed that U(VI) adsorbed at chitosan monolayer coverage area. Also, the chitosan bio-adsorbent was indeed regenerated by 1M $H_2SO_4$ and 1/50 S/L ratio for 75 min of contact. Seven rounds of adsorption-desorption investigations attended to scrutinize the working applicability and renewed application of the bio-adsorbent.

**Keywords**: Chitin; Chitosan; Uranium adsorption; Kinetics; Regeneration

## 1. INTRODUCTION

Chitin is a thick, inelastic, white, nitrogenous polysaccharide seen in the interior structure and exoskeleton of invertebrates [1]. Chitosan (CS) is produced from chitin that is economically attainable. Chitin and CS were observed as supporting matters in various terrestrial, aquatic, and some microorganisms [2]. CS has unique assets as nontoxicity, biodegradability, and biocompatibility [3]. Chitin is comprised of D-glucosamine units and acetyl glucosamine coupled together β-(1-4) glycosidic bonds. Acetyl glucosamine units are dominant in the polymeric series [4]. Chitin deacetylation gives chitosan. It becomes of great importance as an untapped supply and also a unique functional biomatter by the great potential in many provinces [5]. CS was also used for many applications as an adsorbent. It was used to remove metal ions from wastewater [6,7] and dyes [8].

Uranium is an influential nuclear fuel popularly done in nuclear energy and military manufacturing because it could give enormous energy after uranium fission. The recovery and adsorption of uranium(VI) have shown important study content worldwide. Uranium ions were dissolution from rock types by acids or bases to make a leach solution. Uranium ions were generally separated utilizing ion-exchange solid materials and solvent extraction techniques [9-12]. Recently, the adsorption techniques applied to examine uranium ions' separation. Uranium ions were adsorbed as the anionic varieties $[UO_2(SO_4)_3]^{4-}$ and $[UO_2(SO_4)_2]^{2-}$ by solid adsorbents such as Ambersep 920 Cl, Duolite ES-467, aminophosphonic resins, and activated carbon (AC) impregnated trioctyl phosphine oxide [13-16].

Numerous polymers and adsorbent beads were impregnated by organic solvents to adsorb metal ions. Amberlite XAD-16 functionalized

by pyridylazoresorcinol was operated for U(VI) adsorption [17]. Similarly, a CS polymer was reacted with aminotriazole thiol to produce CS/azole resin that was utilized for uranium ions separation [18]. Furthermore, CS-modified titanium dioxide was manufactured to eliminate uranium and europium ions from solutions [19], polyvinylpyrrolidone/CS was utilized for the elimination of U(VI) [20]. Coupling CS with aminonaphthol sulfonic acid to become a brilliant synergistic influence of aminonaphthol sulfonic/CS employed to remove thorium ions [21]. U(VI) adsorption was deliberated by chitosan phosphate to attain information of U(VI) elimination in liquid systems, exclusively seawater and mine wastewater [22].

CS is identified to possess the highest adsorption capability for several heavy metals. In reality, CS was noted to possess a large current for combining with metal ions when comparing with different biopolymers [23]. This action is raised from the attendance of –OH, -$NH_2$ and -NH groups on CS backbone, which originates superior chelation and adsorbing bi-polymer toward toxic and valuable metal ions [24]. U(VI) is basically attached to -OH and amine groups of -CH polymer within ion exchange and chelation reaction [25]. CS bio-adsorbent was operated to purify water, particularly underground water and natural water contaminated with radioactive substances [26]. CS was also utilized for U(VI) deletion from wastewater [27]. Recently, various different classes of CS designated for wastewater remediation were exhibited in kind of films, microcapsules, nanoparticles, and nanofibers [28-31] to improve its potential adsorption applications.

The purpose of this examination was to make chitosan from chitin by the deacetylation method. CS was appropriated to eliminate U(VI) from the uranyl sulfate solution. The different conditions, as pH, temperature, time of contact, and initial U(VI) concentration, were determined through batch technique.

## 2. EXPERIMENTAL

### *2.1. Materials*

Chitin (99%) was acquired from Haihang Industry CO., LTD, Shandong, China. Arsenazo III (99%), ferrous sulfate, sodium nitrite, sodium hydroxide, and ammonium vanadate attained from Merch, Germany. Methanol and ethyl acetate acquired from Scharla, Spain.

A solution of uranyl sulfate (1000 mg/L) was set by solubility a 1.782 g of uranyl acetate dihydrate (99%, Merck, Germany) in 100 mL of deionized $H_2O$ developed by the increment of 50 mL $H_2SO_4$ (98%) and then dilution with deionized $H_2O$ to a suitable volume.

### *2.2. Chitosan preparation*

Chitin deacetylation [31, 32] was done to gain CS via stirring 20 g of chitin in 100 mL 50% NaOH. The mixture was frozen down and retained at -85 °C in the ultra-freezing for 28 hours. Afterward, the mixture's temperature was elevated to 112 °C, with stirring at 275 rpm for 8 hours. Chitosan was gained, filtrated, washed with deionized $H_2O$ until pH7, and dried in a vacuum furnace at 65 °C.

### *2.3. Instruments and adsorbent characterization*

U(VI) were assessed by double at JENWAY UV/Vis 6405 spectrophotometer at 655.0 nm with 1cm quartz cells, cover the UV/visible range 200–1100 nm using Arsenazo III that employed as color-complex with U(VI) [33]. Moreover, XRD was done to scrutinize the variations in the mineralogical composition, and it gained from Bruker Co. model D8. Furthermore, a SEM-EDX was adopted to designate the shape of chitosan before and afterward adsorption. It attained from Philips XL 30. Surface area, and pore size and volume before and afterward adsorption were measured by BET analyzer model Nova Touch LX2 (USA). CS was also described via FTIR (Prestige–21 Shimadzu IR) regulated by Software of IR resolution.

### *2.4. Adsorption procedures*

To study U(VI) adsorption, several attempts were conveyed to gain the excellent parameters that are pH, initial concentration, time of contact, and temperature. The adsorption investigations were offered by associating 50 mL solution of different initial uranium

concentrations with 50 mg adsorbent dose in 100 mL conical flasks at180 rpm mechanical shaker and different time of contact altering from 5 -120 min at various temperatures. Moreover, pH was reconnoitered by extending from 1-6, whereas pH was regulated by 1M NaOH and/or 1M $H_2SO_4$. After filtration, uranium ions uptake was calculated. All the attempts were executed in triplicate, and its mean assessment was done in all cases. Adsorption capacity $q_{eq}$ (mg/g), adsorption efficiency ($E_{ad}$, %), and adsorption constant ($K_d$) appraised from the subsequent equations:

$$q_{eq} = \left(C_i - C_{eq}\right)\frac{V}{m} \quad (1)$$

$$E_{ad}(\%) = \left(\frac{C_i - C_{eq}}{C_i}\right)100 \quad (2)$$

$$K_d = \left(\frac{C_i - C_{eq}}{C_{eq}}\right)\frac{v}{m} \quad (3)$$

Where $C_i$ and $C_{eq}$ are the initial and equilibrium concentrations (mg/L). $V$ (L), and $v$ (mL) are the solution volume, and m is the bio-adsorbent mass (g).

## 3. RESULTS AND DISCUSSION

### *3.1. Description of the prepared bio-adsorbent*

The XRD shapes of chitosan (CS) before and after U(VI) adsorption were demonstrated in Fig. 1a,b. According to manifest in Fig. 1a, , the characteristic peaks of CS exhibited a major broad peak at 2θ = 19° that conform to the database of Bruker software COD 7114110, 7150157, 8100678. For the XRD pattern of U/CS (Fig. 1b), some new peaks were observed after adsorption via the database of Bruker software COD 8103695. In contrast, the peaks intensities were slightly changed,indicating that the CS crystallinity does not imply alteration after U(VI) adsorption.

The SEM was also appropriated to reconnoiter the variation of surface and physical formations of CS and U/CS as exhibited in Fig. 1c,d. The CS surface has smoothly formed by several holes, as disclosed in Fig. 1c. After U(VI) adsorption on CS, SEM picture point to the pores filled with U(VI), and also the surfaces were irregular and agglomerated particles with bigger interstitial holes (Fig. 1d). The semi-quantitative analysis of CS and U/CS gained in EDX spectrums (Fig. 1e,f). The results in Fig. 1e, nitrogen, carbon, and oxygen peaks were existent in CS spectrum. After uranium ions adsorption on the CS bio-adsorbent (U/CS), it was clearly observed in Fig. 1f, that were distinct peaks of uranium ions on the spectrum. The uranium peaks were perceived and confirmed U(VI) adsorption on CS.

The Brunner-Emmett-Teller analyzer (BET) is done to assess solid or porous materials surface area. $N_2$ sorption-desorption analyzer utilized to assess surface area, pore-volume, and pore-size of the studied materials. Fig. 2a,b displayed the $N_2$ sorption-desorption isotherm patterns of CS and U/CS. From the obtained information in Table 2a, surface area, pore-volume, and pore-size of CS were 19.77 $m^2/g$, 0.033 cc/g, 2.65 nm, respectively. On the conflicting, after uranium ions adsorption, the surface area (17.61 $m^2/g$), and pore-volume (0.031 cc/g), pore-size (2.55 nm) of U/CS were decreased according to pore-blocking with U(VI). The attained consequences exposed that U(VI) powerfully adsorbed on CS.

FTIR technique was utilized to identify several unique functional groups standing at CS bio-adsorbent surface. The CS spectrum in Fig. 2c observed a broad peak around 3200-3550 $cm^{-1}$ that submitted to -OH groups overlapping with -NH, $-NH_2$ groups [34, 35]. The classical peaks at 2915 $cm^{-1}$ and 2865 $cm^{-1}$ allocated to $-CH_2$ groups. The distinctive peak (1646 $cm^{-1}$) related toward $-NH_2$, and 1434 $cm^{-1}$ matched toward –NH deformation peak [36]. The peak (1550 $cm^{-1}$) fitted to C = N, while peaks (1166 $cm^{-1}$ and 1018 $cm^{-1}$) fitted to C-N stretching [37]. Besides, the peaks (1373 and 1311 $cm^{-1}$) recognized to C-O and C-O-C stretching vibration. The absorption peak (894 $cm^{-1}$) corresponded to d-glucose unit's characteristic absorption [38]. The provided information in

Fig. 2d, it showed the principal alterations among the beyond data and after U(VI) adsorption at CS bio-adsorbent. After adsorption, the –OH, -NH, C-O, and C=N stretching peaks for CS moved to redshift by 5-10 $cm^{-1}$, which might attitude to U(VI) pickup at CS surface. Moreover, the new peaks of O=U=O were 974 and 894 $cm^{-1}$ [39, 40] of U/CS. Additionally, two weak peaks of U–O were near the ≈ 465 and ≈ 425 $cm^{-1}$ [41]. Hence, the uranyl cations reacted with -$NH_2$, -NH, -OH, and epoxy groups. Accordingly, it realized that the CS was more friendly to adsorb U(VI).

**Table 1**. Surface area, pore-volume, and pore-size of CS and U/CS.

| | Surface area, ($m^2$/g) | Pore-volume, (cc/g) | Pore-size, (nm) |
|---|---|---|---|
| **CS** | 19.77 | 0.033 | 2.65 |
| **U/CS** | 17.61 | 0.031 | 2.55 |

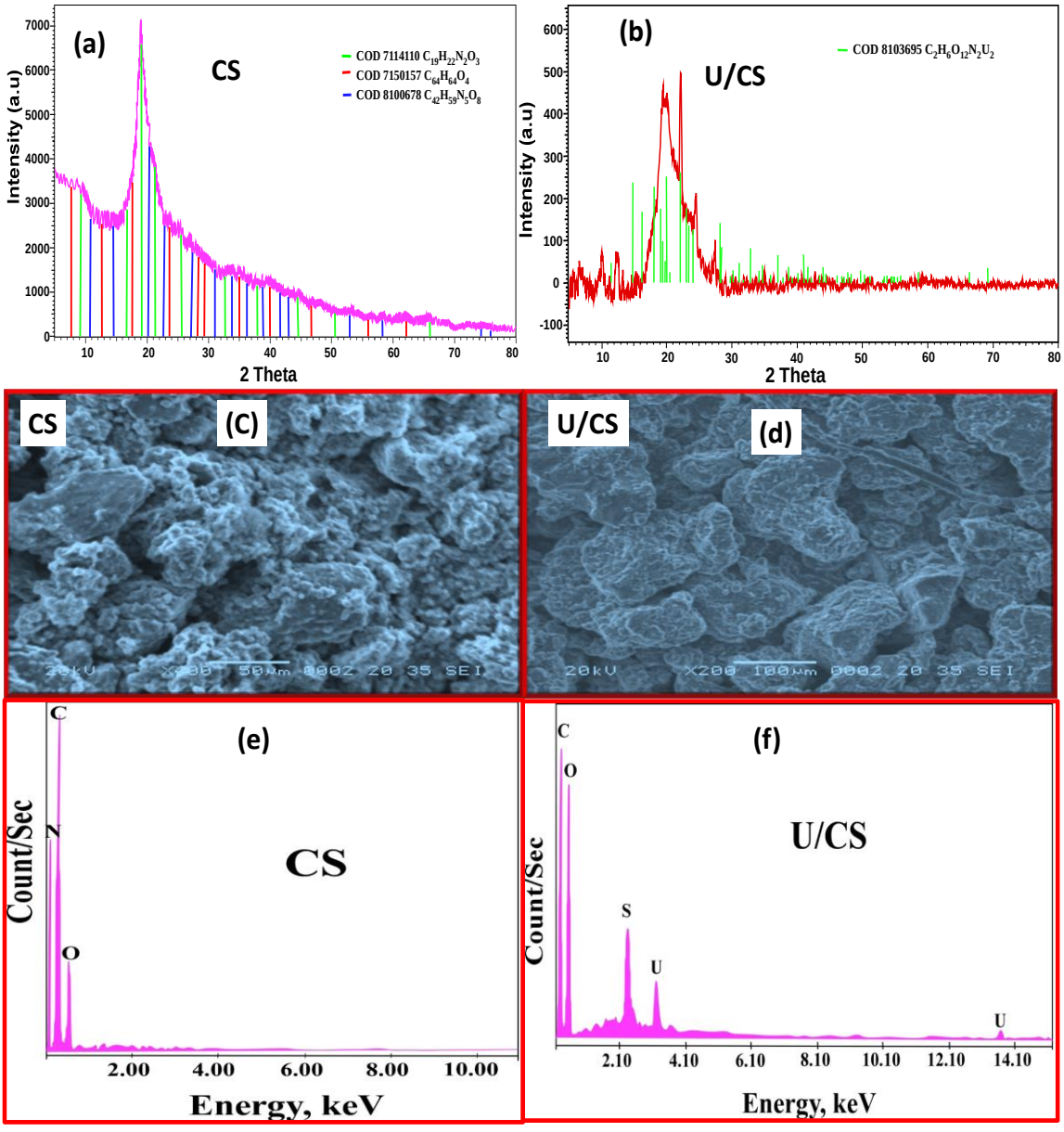


**Fig. 1**. XRD of (a) CS, and (b) U/CS; SEM of (c) CS, and (d) U/CS; EDX of (e) CS, and (f) U/CS.

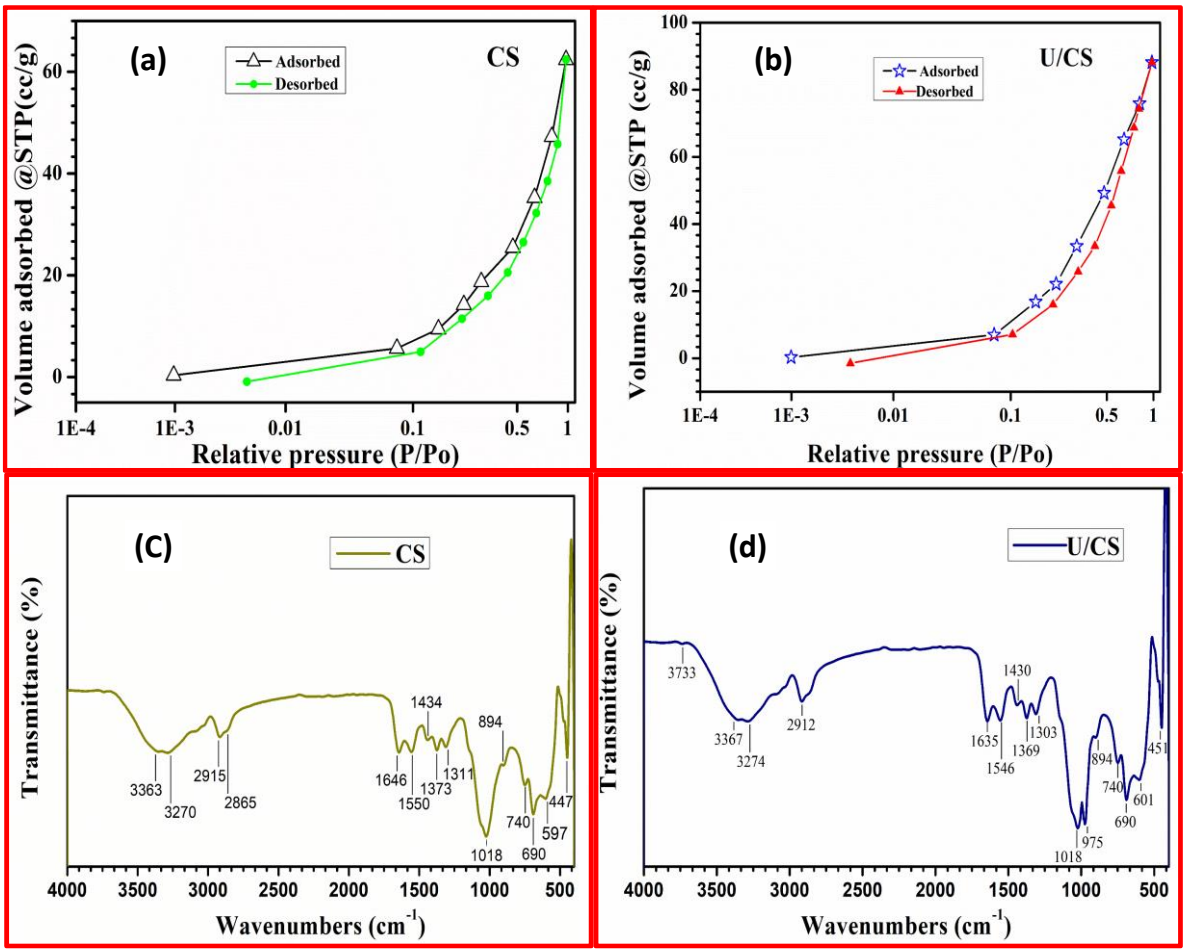


**Fig. 2**. $N_2$ sorption/desorption of (a) CS, and (b) U/CS; FTIR of (c) CS, and (d) U/CS.

### *3.2. Adsorption studies*

Chitosan was utilized for U(VI) adsorption from $H_2SO_4$ solution. It explores uranium ions' adsorption efficiency to estimate the best conditions that are pH, temperature, time of contact, and initial concentration.

#### *3.2.1. Influence of pH*

The pH is an imperative factor that organized sorbate adsorption procedures. The pH impact on U(VI) adsorption from uranyl sulfate solution could exhibit in Fig. 3. Numerous trials were carried out at several pH varieties from 1 to 6. Simultaneously, the other conditions were kept constant at 50 mL volume, assessing U(VI) (200 mg/L), 50 mg bio-adsorbent dose for 30 min time and room temperature. The achieved data in Fig. 3, U(VI) adsorption efficiency was regularly augmented from 2.0 - 37.5% through growing pH from 1 - 3.5, conversely U(VI) adsorption efficiency diminished to 6.0% by rising the pH to 6.0 value. At optimum pH 3-4, U(VI) exists in cationic species ($UO_2^{2+}$, dimmer $((UO_2)_2(OH)_2)^{2+}$, trimmer $((UO_2)_3(OH)_5)^{+}$) [41]. Adsorption uptake was reduced in solution owing to majority of bisulfate ($HSO_4^-$) ions that have a great facility to adsorb on the active sites of the CS adsorbent. So these ions competed with the uranium anion complexes during adsorption processes. The concentration of bisulfate ions was reduced with growing pH, and the adsorption uptake was improved till the extreme adsorption at pH 3.5. At the pH>3.5, the lower U(VI) adsorption was detected; this might designate that some amount of U(VI) ions are precipitated as sodium diuranate form. Consequently, pH 3.5 was nominated as an optimum pH.

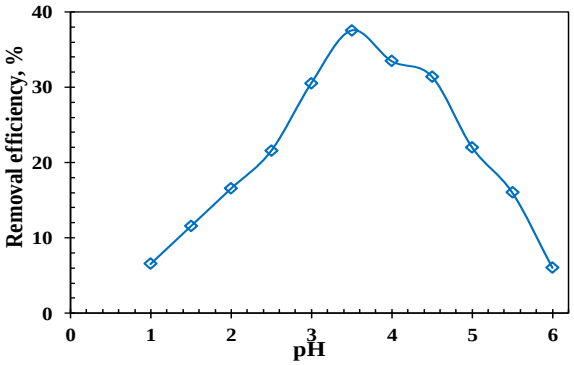


**Fig. 3.** pH influence on U(VI) adsorption efficiency using CS bio-adsorbent (50 mL volume, 200 mg/L U(VI), 50 mg adsorbent dose, 30 min time, 25 °C).

### *3.2.2. Influence of contacting time*

Impact of contacting time was intended on U(VI) adsorption efficiency at CS by ranging 5 - 120 min. In dissimilarity, the further parameters were permanent at pH 3.5, 50 mg CS dose, 50 mL volume, 200 mg/L U(VI) and 25 °C. As realized in Fig. 4, U(VI) adsorption efficiency increased with growing the time until it reached equilibrium at 50 min but the no change of adsorption efficiency by increasing contact time more than 50 min. Therefore, the equilibrium contact time was 50 min for additional work.

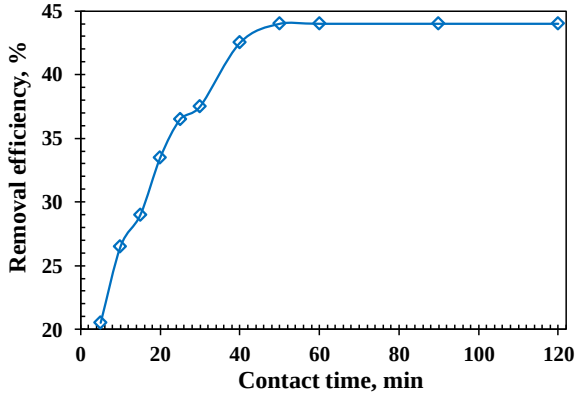


**Fig. 4.** Time of contact influence at U(VI) adsorption efficiency using CS bio-adsorbent (50 mL volume, 200 mg/L U(VI), pH 3.5, 50 mg CS dose, 25 °C).

### *3.2.3. Influence of U(VI) concentration*

Initial sorbate concentration influence is the crucial parameter on adsorption system, and it may upset the adsorption achievement of uranium ions. Numerous batch assessments were practical for observation U(VI) concentration result on its adsorption efficiency via 50 mg CS dose. These tests were performed by shaky 50 mL of different U(VI) concentration ranged of 25 - 600 mg/L, pH 3.5 for 50 min time at 25 °C. In Fig. 5, U(VI) concentration was raised, and adsorption efficiency reached maximum adsorption at 200 mg/L concentration. The most favorable adsorption at 200 mg/L concentration was 44.0 % to CS bio-adsorbent. Likewise, the uranium maximum loading capacity on CS adsorbent was 88.0 mg/g (Fig. 5). The uptake was kept constant after 200 mg/L. It was stated that the functional CS bio-adsorbent groups arrived the saturation capacity whenever U(VI) mobility was the highest in solution, and whole active sites of CS filled and plugged with U(VI). Therefore, the best U(VI) uptake on CS was 88.0 mg/g.

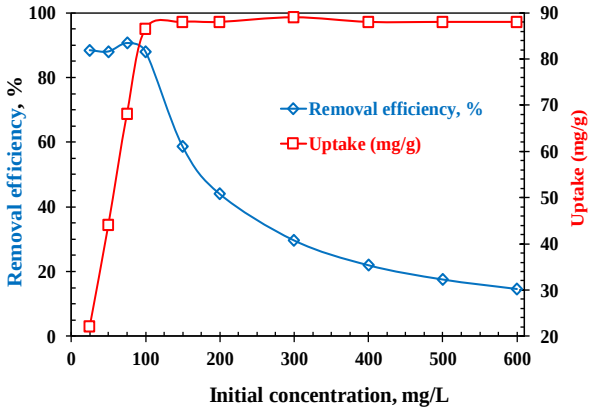


**Fig. 5.** Influence of U(VI) concentration on efficiency and uptake using CS bio-adsorbent (50 mL volume, pH 3.5, 50 mg CS dose, 50 min time, 25 °C).

### *3.2.4. Temperature influence*

The temperature influence on U(VI) adsorption inspected in the temperature extended 25 -55 °C (Fig. 6). The adsorption was also reduced of 44.0 to 42.8 % with rising the temperature to 55 °C. However, rising the temperature leads to Van der Waals bonds' breakdown, and hereafter, the active sites were decreased. Consequently, room temperature was the excellent temperature for U(VI)' adsorption.

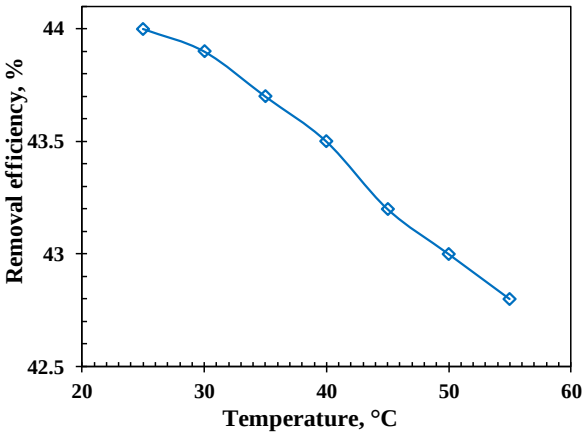


**Fig. 6.** Temperature impact on U(VI) adsorption by CS bio-adsorbent (50 mL volume, 200 mg/L U(VI), pH 3.5, 50 mg CS dose, 50 min time).

### *3.2.5. Kinetic evaluation*

Kinetic designs were investigated to decide the adsorption mechanism forms and the rate-controlling steps. Pseudo–1st–order and pseudo-2nd-order designs employed to find U(VI) adsorption mechanism on CS bio-adsorbent. The 1st-order model [42, 43] performed in linear mode as the resulting equation:

$$\log\left(q_{eq} - q_t\right) = \log q_{eq} - \left(\frac{k_1}{2.303}\right)t \qquad (4)$$

Where $q_{eq}$ also $q_t$ (mg/g) are equilibrium uptake and also at time $t$ (min), and $k_1$ (min$^{-1}$) is the rate constant. The relation of $\log(q_{eq}-q_t)$ and $t$ offer to compute the $k_1$ and $q_e$ from the slope ($k_1$/2.303) and intercept ($\log q_{eq}$). The outcomes in Fig. 7a and Table 2 disclosed that $q_{eq}$ and $R^2$ of adsorption system not appropriate a 1st-order kinetic. Hence, U(VI) adsorption vs. CS was not suitable for this reaction.

On the contrary, the 2nd-order model was fulfilled and assembled in the ensuing equation [44]:

$$\frac{t}{q_t} = \frac{1}{k_2 q_{eq}^2} - \left(\frac{1}{q_{eq}}\right)t \qquad (5)$$

Where $k_2$ (g/mg.min) is the rate constant, $q_t$ (mg/g) the U(VI) uptake at time $t$ (min). This design could forecast the kinetic achievement of adsorption via chemical adsorption method that was the rate-determining stage. The relation of $t/q_t$ vs. $t$ gain straight line when the 2nd-order reaction could be valid. As the information in Fig. 7b and Table 2, the correlation coefficient, $R^2$ was near to unity, and the calculated value of adsorbed amount at equilibrium ($q_{cal}$) was closer to the practical capacity ($q_{exp}$) for the CS bio-adsorbent. These

**Table 2.** Kinetic factors of U(VI) uptake on CS bio-adsorbent.

| Practical uptake, $q_{exp}$ | 1st-order | | | 2nd-order | | |
|---|---|---|---|---|---|---|
| 88 mg/g | $q_{eq}$ (mg/g) | $k_1$ (1/min) | $R^2$ | $q_{eq}$ (mg/g) | $k_2$ (g/mg.min) | $R^2$ |
| | 16.26 | 0.073 | 0.928 | 101.01 | 1.06 x 10$^{-3}$ | 0.986 |

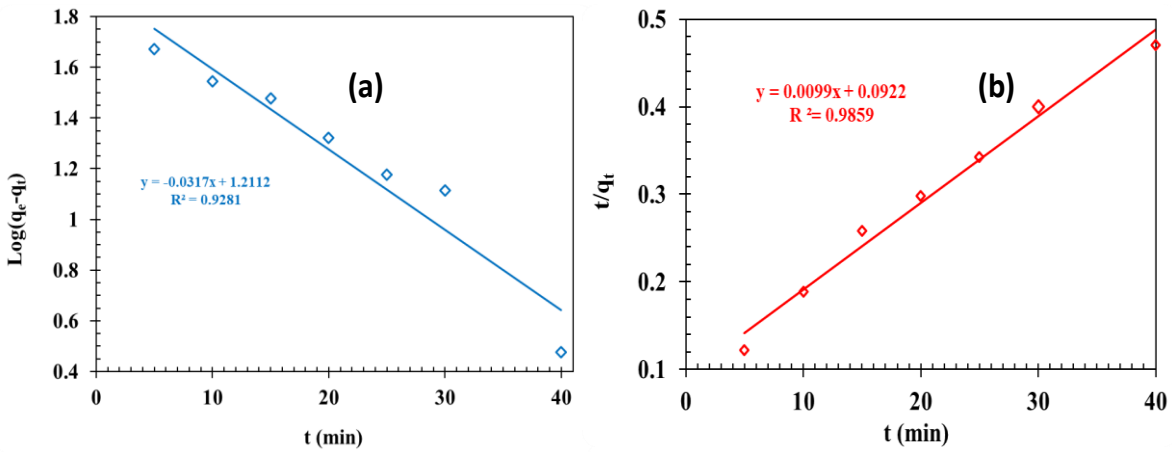


**Fig. 7.** (a) 1st order, and (b) 2nd order models of U(VI) uptake on CS bio-adsorbent.

data advised that U(VI) adsorption at CS bio-adsorbent obeyed well the 2nd-order kinetic.

### *3.2.6. Isotherm studies*

Adsorption isotherms intimate effective systems for the reaction by ion transfer to the adsorbents. It is also a primary requirement for outlining any adsorption operation [45]. The isotherms premeditated to identify various relevant data for adsorption when the adsorbed ions were spread within solid/aqueous phase during the adsorption operation arrived the equilibrium situation. Langmuir and Freundlich models were undertaken to discriminate adsorption techniques. Langmuir model adopted that sorbate uptake was enacted at the homogeneous adsorption facade over monolayer on the CS bio-adsorbent outside with steady energy [46]. The resulting equation was quantified as:

$$\frac{C_{eq}}{q_{eq}} = \frac{1}{q_{\max} b} + \left(\frac{1}{q_{\max}}\right) C_{eq} \qquad (6)$$

Where $q_{max}$ (mg/g) maximum U(VI) uptake, $b$ constant linked to binding sites affinity and energy (L/mg). From the attained data in Fig. 8a and Table 3, the uptake capacity (88.49 mg/g) was closer to practical uptake capacity (88.0 mg/g), also the $R^2$ was closer to unit. The documents clear that U(VI) adsorption monitored Langmuir model.

Freundlich model described U(VI) uptake at CS bio-adsorbent surface. It was commonly utilized to scrutinize surface energies and heterogeneity [47]. Freundlich isotherm was identified as the resulting equation:

$$\log q_{eq} = \log K_f + \left(\frac{1}{n}\right) \log C_{eq} \qquad (7)$$

Where, $K_f$ (mg/g), constant correlated to supreme adsorption uptake, $n$, constant correlated to surface heterogeneity. The curve of $\log q_{eq}$ vs. $\log C_{eq}$ gave a regression line to acquire the $n$ and $K_f$ (Fig. 8b). Freundlich constants $K_f$ and $n$ valued from intercept ($\log K_f$) and slope ($1/n$) (Table 3). The $K_f$ was lesser than U(VI) practical uptake for CS bio-adsorbent. The gotten data exposed that Freundlich model was not acceptable adsorption system.

**Table 3.** The isotherm model factors for U(VI) uptake on CS bio-adsorbent.

| practical uptake, mg/g | Langmuir isotherm | | | Freundlich isotherm | | |
|---|---|---|---|---|---|---|
| 88 | $q_{max}$ (mg/g) | b (L/mg) | $R^2$ | $K_f$ (mg/g) | n (mg.min/g) | $R^2$ |
| | 88.49 | 0.34 | 0.999 | 34.47 | 5.63 | 0.565 |

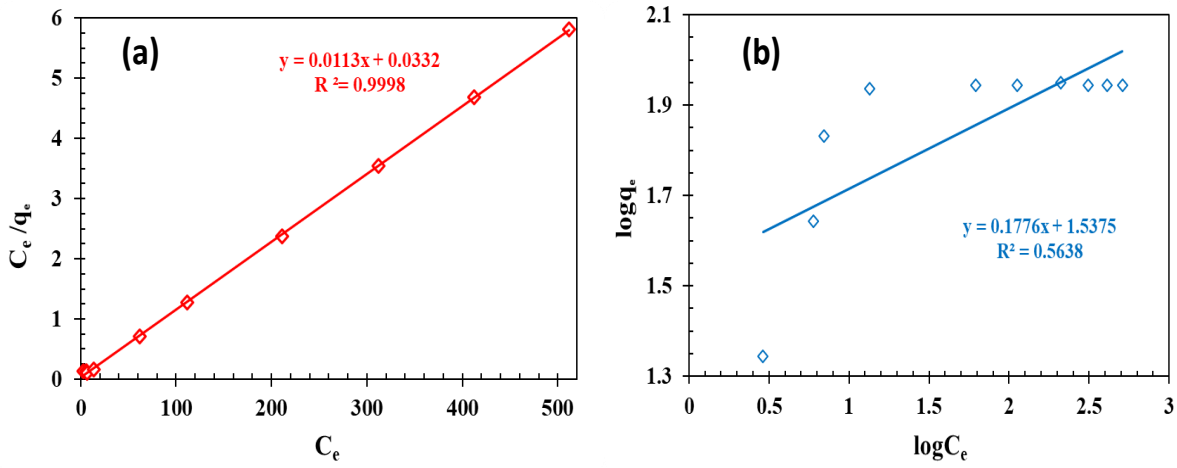


**Fig. 8.** (a) Langmuir, and (b) Freundlich models in U(VI) uptake on CS bio-adsorbent.

### *3.2.7. Thermodynamic characteristics*

Several adsorption trails at different temperature were employed to appraise the thermodynamic conditions as a change in free energy (*ΔG°*, kJ/mol), change in enthalpy (*ΔH°*, kJ/mol), and change in entropy (*ΔS°*, J/mol.K). Adsorption constant, $K_d$, was gotten from the experimental data. Thermodynamic conditions for U(VI) adsorption by CS bio-adsorbent were valued according to Van't Hoff equations [48].

$$\Delta G^\circ = \Delta H^\circ - T\,\Delta S^\circ \quad (8)$$

$$Log K_d = \frac{\Delta S^\circ}{2.303R} - \frac{\Delta H^\circ}{2.303RT} = \quad (9)$$

Where *R* (8.314 J/mol.K) universal gas constant, and *T* (K) absolute temperature. The thermodynamic conditions of CS bio-adsorbent were evaluated from Fig. 9. *ΔH°* and *ΔS°* prepared from the slope (*ΔH°*/2.303*R*) and intercept (*ΔS°*/2.303*R*) (Table 4). The acquired data, negative assessments of *ΔG°* showed that adsorption system was spontaneous. The negative assessment of *ΔH°* might advise exothermic adsorption. Also, negative assessment of *ΔS°* set the feasibility and randomness of adsorption at CS bio-adsorbent/acid solution boundary.

### *3.3. Adsorption mechanism*

The information gained through XRD, SEM-EDX, surface analysis, and FTIR before and afterward adsorption was offered precious report supported assuming adsorption mechanism of U(VI) on CS bio-adsorbent. The XRD pattern for CS bio-adsorbent gained in Fig. 1a, b. The peak positions and peak shape of CS with high intensity at 2θ = 19°. In XRD of U/CS (Fig. 1b), some new peaks were detected due to uranium ions' adsorption on the studied adsorbent. From the SEM (Fig. 1d), the pores were occupied with U(VI), and CS surface was irregular and agglomerate with U(VI). After uranium ions adsorption on CS bio-adsorbent, it detected from the corresponding EDX spectra (Figs. 1f). The uranium peaks were existed and confirmed that uranium ions were adsorbed in the CS surfaces.

The information in Figs. 2a,b, the surface area, pore-size, and pore-volume of CS reduced after U(VI) adsorption according to pore-filling with U(VI). The attained outcomes exposed that U(VI) powerfully adsorbed per CS bio-adsorbent. The FTIR of CS before and afterward U(VI) adsorption (Fig. 2c,d) validated that new peaks of (O=U=O) appear near the 974 and 894 $cm^{-1}$ [39, 40]. Moreover,

**Table 4.** Thermodynamic limits of U(VI) uptake on CS bio-adsorbents.

| **Δ*H°*, (kJ.mol$^{-1}$)** | **Δ*S°*, (kJ.mol$^{-1}$.K$^{-1}$)** | **Temperature, (K)** | | | | | | |
|---|---|---|---|---|---|---|---|---|
| | | 298 | 303 | 308 | 313 | 318 | 323 | 333 |
| -3.63 | -0.95 x $10^{-2}$ | **Δ*G°*, (kJ.mol$^{-1}$)** | | | | | | |
| | | -0.787 | -0.739 | -0.692 | -0.644 | -0.596 | -0.549 | -0.501 |

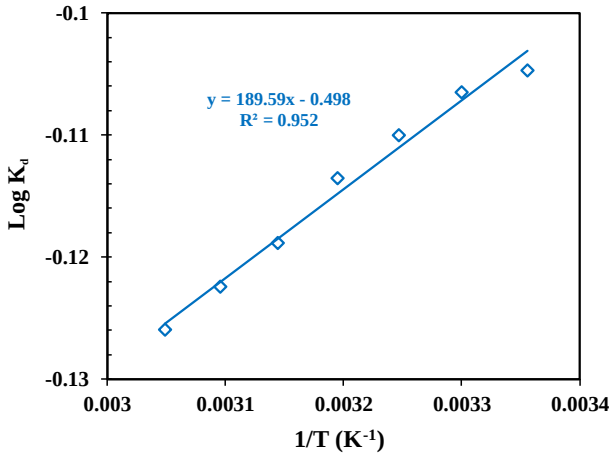


**Fig. 9.** Relation of temperature and adsorption constant for U(VI) uptake on CS bio-adsorbent.

two weak peaks of U–O appear near the ≈ 465 and ≈ 425 $cm^{-1}$ [41] of CS bio-adsorbent. Hence, the uranyl cations react with -$NH_2$, -NH, -OH, and epoxy groups.

The solution pH effect expressed an extra demonstration of adsorption mechanism (Fig. 3 U(VI) binding mechanism may occur out of the functional group's de-protonation of CS bio-adsorbent. At optimal pH 3-4, U(VI) exists in cationic species ($UO_2^{2+}$, dimmer $((UO_2)_2(OH)_2)^{2+}$, trimmer $((UO_2)_3(OH)_5)^{+}$) [41]. The active sites on adsorbent surfaces are hydroxyl, epoxy, -NH, and -$NH_2$ groups; these active sites tended to relate with uranyl ions. Active sites de-protonation and establishment of various uranium hydrolysis products were highly adsorbed due to electrostatic attraction and complexation systems. The kinetic information proposed that U(VI) adsorption fitted further suitably by the 2nd-order model. It specified that adsorption mechanism controlled with chemisorption. At isotherm investigation, Langmuir model displayed brilliant fit for practical data. Besides, the adsorption manner was spontaneous, randomness, and exothermic according to thermodynamics documents. U(VI) form complexes with active sites of CS from the discussion to the beyond analysis. The representation diagram of the U(VI) possible adsorption mechanism onto the CS surface was offered and showed (Fig. 10).

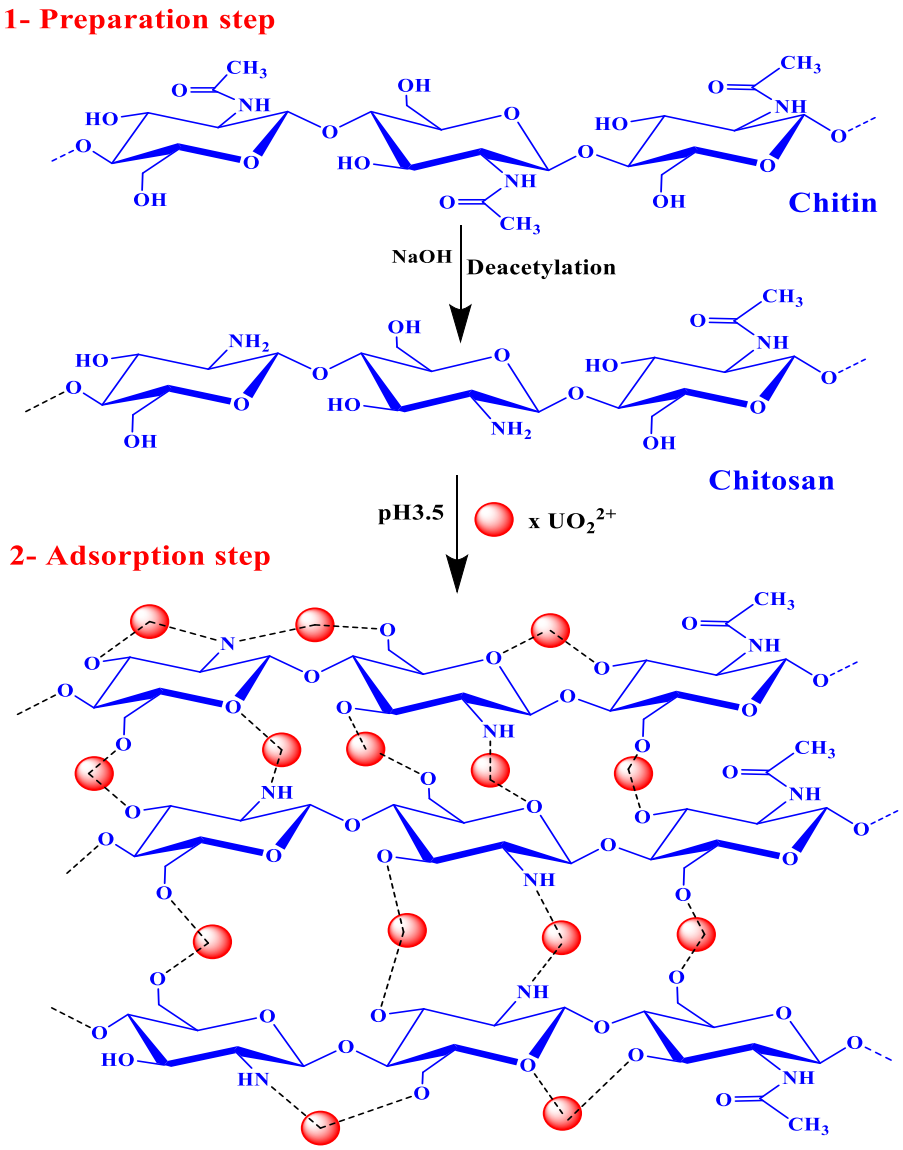


**Fig. 10.** The suggested reaction for CS and uranium cation interactions.

### *3.5. Reusability of CS bio-adsorbent*

Regeneration was applied on uranium-loaded-CS for the reusable several times. To reuse and recycle CS bio-adsorbent, the U/CS were regenerated via 1M $H_2SO_4$ and 1/50 S/L phase ratio for 75 min contacting time. Adsorption-desorption manners were recurrent many stages till desorption efficiency was reduced from 94.0 to 77.0% for the CS adsorbent after seven consecutive series (Table5). It was designated that good adsorption constancy of CS bio-adsorbent with U(VI).

**Table 5.** The efficiency of uranium ions adsorbed and desorbed as a function of the adsorption-desorption cycle. Adsorption cycle: 50 mL volume, 200 mg/L of U(VI), pH 3.5, 50 mg CS dose, 50 min adsorbing time, 25 °C; desorption cycle: 1M $H_2SO_4$ and 1/50 S/L phase ratio for 75 min desorption time at room temperature.

| Number of Cycle | Adsorption (%) | Desorption (%) |
|---|---|---|
| 1 | 44.5 | 94.0 |
| 2 | 43.4 | 93.3 |
| 3 | 42.8 | 92.7 |
| 4 | 41.3 | 88.5 |
| 5 | 39.5 | 85.1 |
| 6 | 37.4 | 82.2 |
| **7** | **35.9** | **77.0** |
| 8 | 23.6 | 67.3 |
| 9 | 20.8 | 62.4 |
| 10 | 18.4 | 55.6 |

## 4. CONCLUSION

The chitin-derived chitosan was employed to U(VI) separation from $H_2SO_4$ solution. The adjusted settings were realized by 50 mL volume, 200 mg/L U(VI) and 50 mg CS dose at pH 3.5 for 50 min time of contact. The realized supreme uptake of CS bio-adsorbent achieved 88.0 mg/g. Furthermore, thermodynamic studies were scrutinized the negative values of $\Delta S°$ and $\Delta H°$ that established a randomness and exothermic, but $-\Delta G°$ indicated spontaneous of U(VI) adsorption at CS bio-adsorbent. Also, kinetic indications stated to fit within 2nd-order kinetic. The consequences confirmed that Langmuir model fitted well at describing adsorption processes. Also, CS bio-adsorbent was certainly regenerated by 1M $H_2SO_4$ and 1/50 S/L ratio for 75 min time. Adsorption-desorption processes were recurring various stages up until desorption efficiency reduced for CS bio-adsorbent after seven consecutive times. It was designated good adsorption of U(VI) on the chitosan bio-adsorbent.

## REFERENCES

[1] Shamshina JL, Berton P, Rogers RD. Advances in functional chitin materials: a review. ACS Sustain. Chem. Eng. 2019; 7(7):6444–6457. https://doi.org/10.1021/acssuschemeng.8b06372 .

[2] Muzzarelli RAA, Boudrant J, Meyer D, Manno N, DeMarchis M, Paoletti MG. Current views on fungal chitin/chitosan, human chitinases, food preservation, glucans, pectins, and inulin: a tribute to Henri Braconnot, precursor of the carbohydrate polymers science, on the chitin bicentennial. Carbohydr. Polym. 2012; 87(2):995-1012. https://doi.org/10.1016/j.carbpol.2011.09.063.

[3] Kurita K. Chitin and chitosan: functional biopolymers from marine crustaceans. Mar. Biotechnol. 2006; 8(3):203. https://doi.org/10.1007/s10126-005-0097-5.

[4] Zamani A, Jeihanipour A, Edebo L, Niklasson C, Taherzadeh MJ. Determination of glucosamine and N-acetyl glucosamine in fungal cell walls. J. Agric. Food Chem. 2008; 56(18):8314–8318. https://doi.org/10.1021/jf801478j.

[5] Dutta PK, Dutta J, Tripathi V. Chitin and chitosan: chemistry, properties, and applications. J. Scientific & Industrial Res. 2004; 63:20-31.

[6] Perumal S, Atchudan R, Yoon DH, Joo J, Cheong IW. Spherical chitosan/gelatin hydrogel particles for removal of multiple heavy metal ions from wastewater. Ind. Eng. Chem. Res. 2019; 58(23):9900-9907. https://doi.org/10.1021/acs.iecr.9b01298.

[7] Zargar V, Asghari M, Dashti A. A review on chitin and chitosan polymers: structure, chemistry, solubility, derivatives, and applications. ChemBioEng Rev. 2015; 2(3):204-226. https://doi.org/ 10.1002/cben .201400025.

[8] Le HQ, Sekiguchi Y, Ardiyanta D, Shimoyama Y. $CO_2$-activated adsorption: a new approach to dye removal by chitosan hydrogel. ACS Omega 2018; 3(10):14103-14110. https://doi.org/10.1021/acsomega.8b01825.

[9] Atia B, Gado M, Cheira M. Kinetics of uranium and iron dissolution by sulfuric acid from Abu Zeneima ferruginous siltstone, southwestern Sinai, Egypt. Euro-Mediterr. J. Environ. Integr. 2018; 3:39. https://doi.org/10.1007/s41207-018-0080-y.

[10] Sakr AK, Mohamed SA, Mira HI, Cheira MF. Successive leaching of uranium and rare earth elements from el Sela mineralization. J. Sci. Eng. Res. 2018; 5:95–111. https://jsaer.com/archive/volume-5-issue-9-2018/.

[11] Zakia SA, Rashad MM, Mohamed SA, Elsheikh EM, Mira HE, Abd El Wahab GM. Kinetics of uranium leaching process using sulfuric acid for Wadi Nasib ore, South western Sinai, Egypt. Aswan Univ. J. Environ. Studies 2020; 1:171-182. doi: 10.21608/AUJES. 2020. 127584.

[12] Cheira MF. Solvent extraction of uranium and vanadium from carbonate leach solutions of ferruginous siltstone using cetylpyridinium carbonate in kerosene. Chem. Papers 2020; 74:2247–2266. https://doi.org/10.1007/s11696-020-01073-w.

[13] Cheira MF, El-Didamony AM, Mahmoud KF, Atia BM. Equilibrium and kinetic characteristics of uranium recovery by the strong base Ambersep 920U Cl resin. IOSR-Appl. Chem. 2014; 7:32-40. doi:10.9790/5736-07533240.

[14] Zidan IH, Cheira MF, Bakry AR, Atia BM. Potentiality of uranium recovery from G. Gattar leach liquor using Duolite ES-467 chelating resin: Kinetic, thermodynamic and isotherm features. Intern. J. Environ. Anal. Chem. 2020; 1-23. https://doi.org/10.1080/03067319.2020.1748613.

[15] Cheira MF. Characteristics of uranium recovery from phosphoric acid by an aminophosphonic resin and application to wet process phosphoric acid. European J. Chem. 2015; 6:48 - 56. doi:10.5155/eurjchem.6.1.48-56.1143.

[16] Abdien HG, Cheira MF, Abd-Elraheem MA, El-Naser TS, Zidan IH. Extraction and pre-concentration of uranium using activated carbon impregnated trioctyl phosphine oxide. Elixir Appl. Chem. 2016; 100:3462-43469. https://www.elixirpublishers.com/articles/1480509836_ELIXIR2016095352.pdf.

[17] Cheira MF. Synthesis of pyridylazo resorcinol-functionalized Amberlite XAD-16 and its characteristics for uranium recovery. J. Environ. Chem. Eng. 2015; 3:642-652. https://doi.org/10.1016/j.jece.2015.02.003.

[18] Atia AA. Studies on the interaction of mercury II and uranyl II with modified chitosan resins. Hydrometallurgy 2005; 80:13-22. https://doi.org/10.1016/j.hydromet.2005.03.009.

[19] Wang J, Huo Y, Ai Y. Experimental and theoretical studies of chitosan modified titanium dioxide composites for uranium and europium removal. Cellulose 2020; 27:7765–7777. https://doi.org/10.1007/s10570-020-03337-w.

[20] Christou C, Philippou K, Krasia-Christoforou T, Pashalidis I. Uranium adsorption by polyvinylpyrrolidone/chitosan blended nanofibers. Carbohydrate Polymers 2019; 219:298–305. https://doi.org/10.1016/ j.carbpol.2019.05.041.

[21] Gado MA, Atia BM, Cheira MF, Abdou AA. Thorium ions adsorption from aqueous solution by amino naphthol sulphonate coupled chitosan. Intern. J. Environ. Anal. Chem. 2019; 1-18. https://doi.org/10.1080/03067319.2019.1683552.

[22] Sakaguchi T, Horikoshi T, Nakajima A. Adsorption of uranium by chitin phosphate and chitosan phosphate. Agri. Biol. Chem. 1981: 45(10):2191-2195. doi: 10.1080/00021369. 1981.10864862.

[23] Crini G. Recent developments in polysaccharide-based materials used as adsorbents in wastewater treatment. Prog. Polym. Sci. 2005; 30:38-70. https://doi.org/10.1016/j.progpolymsci.2004.11.002.

[24] Fan L, Luo C, Sun M, Li X, Qiu H. Highly selective adsorption of lead ions by water-dispersible magnetic chitosan/graphene oxide composites. Colloids Surf. B: Biointerfaces 2013; 103:523-529. https://doi.org/ 10.1016/j.colsurfb.2012.11.006.

[25] Motawie AM, Mahmoud KF, El-Sawy AA, Kamal HM, Hefni H, Ibrahiem HA. Preparation of chitosan from the shrimp shells and its application for pre-concentration of uranium after cross-linking with epichlorohydrin. Egy. J. Petroleum 2014; 23(2):221-228. https:// doi.org/10.1016/j.ejpe.2014.05.009.

[26] Kang S, Lee J, Kim T, Lee H, Kim J, Kim C, Ko C, Yong-Beom K, Nam-Gi K. Removal of uranium in water system by chitosan beads. Theor. Appl. Chem. Eng. 2003; 9(2):2266.

[27] Yi Z, Li J. Removal of uranium(VI) from aqueous solution by dry chitosan powder. Adv. Mat. Res. 2012; 366:434-437. https://doi.org/10.4028/www.scientific.net/AMR.366.434.

[28] Frantz TS, Silveira N Jr, Quadro MS, ndreazza R, Barcelos AA, Cadaval TRS Jr, Pinto LAA. Cu(II) adsorption from copper mine water by chitosan films and the matrix effects. Environ. Sci. Pollut. Res. Int. 2017; 24(6):5908–5917. https://doi.org/10.1007/s11356-016-8344-z.

[29] Sivakami MS, Gomathi T, Venkatesan J, Jeong HS, Kim SK, Sudha PN. Preparation and characterization of nanochitosan for treatment wastewater. Int. J. Biol. Macromol. 2013; 57:204-212. https://doi.org/ 10.1016/j.ijbiomac.2013.03.005.

[30] Nthunya LN, Masheane ML, Malinga SP, Nxumalo EN, Mhlanga SD. Environmentally benign chitosan-based nanofibers for potential use in water treatment. Cogent Chem. 2017; 3(1):1357865. https://doi.org/10.1080/23312009. 2017.1357865.

[31] Antonino RS, Fook BR, Lima VA, Rached RÍ, Lima EP, Lima RJ, Covas CA, Fook MV. Preparation and characterization of chitosan obtained from shells of shrimp (*Litopenaeus vannamei boone*). Mar. Drugs 2017; 15:141. doi:10.3390/md15050141.

[32] Mohammed MH, Williams PA, Tverezovskaya O. Extraction of chitin from prawn shells and conversion to low molecular mass chitosan. Food Hydrocolloids 2013; 31: 166-171. https://doi.org/10.1016/j.foodhyd.2012.10.021.

[33] Marczenko Z, Balcerzak M. Separation, Preconcentration and Spectrophotometry in Inorganic Analysis. Elsevier Science B.V., Amesterdam, Netherland. 2000; 446-455.

[34] Liu L, Yang W, Gu D, Zhao X, Pan Q. In situ preparation of chitosan/ZIF-8 composite beads for highly efficient removal of U(VI). Front. Chem. 2019; 7:607. doi:10.3389/fchem. 2019. 00607.

[35] Jeon C, Höll WH. Chemical modification of chitosan and equilibrium study for mercury ion removal. Water Res. 2003; 37:4770-4780. https://doi.org/10.1016/S0043-1354(03)00431-7.

[36] Monier M, Elsayed NH. Selective extraction of uranyl ions using ion-imprinted chelating microspheres. J. Colloid Inter. Sci. 2014; 423: 113-122. https://doi.org/10.1016/ j.jcis.2014.02.015.

[37] Sun Z, Chen D, Chen B, Kong L, Su M. Enhanced uranium(VI) adsorption by chitosan modified phosphate rock. Coll. Surf. A: Physicochem. Eng. Aspects 2018; 547:141-147. https://doi.org/10.1016/j.colsurfa.2018.02.043.

[38] Cheira MF. Synthesis of aminophosphonate-functionalised ZnO/polystyrene-butadiene nanocomposite and its characteristics for uranium adsorption from phosphoric acid. Intern. J. Environ. Anal. Chem. 2019; 1-25. https://doi.org/10.1080/03067319.2019.1686493.

[39] Cheira MF, Kouraim, MN, Zidan IH, Mohamed WS, Hassanein TF. Adsorption of U(VI) from sulfate solution using montmorillonite/ polyamide and nano-titanium oxide/polyamide nanocomposites. J. Environ. Chem. Eng. 2020; 8: 104427. https://doi.org/10.1016/j. jece.2020.104427.

[40] Wang G, Liu J, Wang X, Xie Z, Deng N. Adsorption of uranium (VI) from aqueous solution onto cross-linked chitosan. J. Hazard. Mat. 2009; 168:1053–1058. https://doi.org/ 10.1016/j.jhazmat.2009.02.157

[41] Abdien HG, Cheira MF, Abd-Elraheem MA, Saef El-Naser TA, Zidan IH. Removal of uranium from acidic solution using activated carbon impregnated with tributyl phosphate. Biol. Chem. Res. S.S. Pub. 2016; 2016:313-340.http://www.ss-pub.org/wp-content/uploads/ 2016 /11/BCR 2016081701. pdf.

[42] Cheira MF, Rashed MN, Mohamed AE, Hussein GM, Awadallah MA. Removal of some harmful metal ions from wet-process phosphoric acid using murexide-reinforced activated bentonite. Mat. Today Chem. 2019; 14: 100176. https://doi.org/10.1016/j.mtchem.2019.06.002.

[43] Atia BM, Khawassek YM, Hussein GM, Gado MA, El-Sheify MA, Cheira MF. One-pot synthesis of pyridine dicarboxamide derivative and its application for uranium separation from acidic medium. J. Environ. Chem. Eng. 2021; 9:105726.https://doi.org/10.1016/j.jece.2021.105726.

[44] Cheira MF, Rashed MN, Mohamed AE, Zidan IH, Awadallah MA. The performance of Alizarin impregnated bentonite for the displacement of some heavy metals ions from the wet phosphoric acid. Sep. Sci. Tech. 2020; 55: 3072-3088. https://doi.org/10.1080/01496395. 2019.1675701.

[45] Sayed AS, Abdelmottaleb M, Cheira MF, Abdel-Aziz G, Gomaa H, Hassanein TF. Date

seed as an efficient, eco-friendly, and cost-effective bio-adsorbent for removal of thorium ions from acidic solutions. Aswan Uni. J. Environ. Studies 2020; 1:106-124. doi: 10.21608/aujes.2020.124579.

[46] Kadous A, Didi MA, Villemin D. A new sorbent for uranium extraction:ethylenediamino tris-methylene phosphonic acid grafted on poly styrene resin. J. Radioanal. Nucl. Chem. 2010; 284: 431-438. https://doi.org/10.1007/s10967-010-0495-7.

[47] Cheira MF. Performance of poly sulfonamide/nano-silica composite for adsorption of thorium ions from sulfate solution. SN Appl. Sci. 2020; 2:398. https://doi.org/10.1007/s42452-020-2221-6.

[48] Atia BM, Gado MA, Cheira MF, El-Gendy HS, Yousef MA, Hashem MD. Direct synthesis of a chelating carboxamide derivative and its application for thorium extraction from Abu Rusheid ore sample, South Eastern Desert, Egypt. Intern. J. Environ. Anal. Chem. 2021; 1-24. https://doi.org/10.1080/03067319. 2021. 1924161.

# خصائص إمتزاز اليورانيوم من المحلول الحمضي بإستخدام الشيتوزان المشتق من الكيتين كممتز بيولوجي منخفض التكلفة

**خالد علي جاد الله عبد الرحيم [1]، محمود احمد طاهر[1] ، محمد فريد شعيره [2]**

1- قسم الكيمياء ، كلية العلوم جامعة الازهر فرع اسيوط

2- هيئة المواد النووية ، ص . ب المعادي القاهرة

**الملخص العربي :**

في هذا العمل، تم تحضير الشيتوزان منخفض التكلفة (CS) من خلال نزع مجموعات الاستيل من الكيتين بإستخدام هيدروكسيد الصوديوم. وتم توصيف الشيتوزان المحضر بواسطة جهاز إنحراف الأشعة السينية (XRD)، والماسح المجهري الإلكتروني (SEM)، والتحليل الطيفي المشتت للطاقة (EDX)، ومحلل مساحة السطح Brunner-Emmett-Teller (BET) ، وتحويل فوريير الطيفي بالأشعة تحت الحمراء (FTIR). وتم إستخدام الشيتوزان لإمتزاز أيونات اليورانيوم من محلول الكبريتات. وتبين أن الحد الأقصى لإمتزاز أيونات اليورانيوم علي الشيتوزان هو 88.0 مجم/جم عند pH3.5، 200 مجم/لتر تركيز أولي من أيونات اليورانيوم، عند درجة حرارة الغرفة. وتبين أن الدراسات الحركية تتلاءم بشكل جيد مع النموذج الحركي من الدرجة الثانية الكاذبة الذي يفترض أن عملية الامتزاز تحدث كيميائياً. وتحققت عملية الإتزان في غضون 50 دقيقة وتبين أيضًا أن نموذج لانجمير هو الأنسب لعملية أمتزاز أيونات اليورانيوم علي الطبقة الأحادية للشيتوزان. تم أيضًا إعادة تجدد الشيتوزان المحمل بأيونات اليورانيوم بإستخدام 1 مول من حمض الكيريتيك، لمدة 75 دقيقة زمن التلامس. وتبن ان كفاءة عملية الامتزاز تقل بعد سبع دورات من تجارب الامتزاز والاسترجاع. وبالتالي وضحت النتائج أهمية إستخدام الشيتوزان في التطبيق العملي وتكرار هذه العملية. وتبين أيضًا ان عملية الامتزاز بالشيتوزان سهلة وبسيطة وغير مكلفة لإستخلاص اليورانيوم من محاليه المائية.